Thermolubricity in atomic-scale friction

K. B. Jinesh,* S. Yu. Krylov,† H. Valk, M. Dienwiebel,‡ and J. W. M. Frenken§
Kamerlingh Onnes Laboratory, Leiden University, P.O. Box 9504, 2300 RA Leiden, The Netherlands
(Received 29 April 2008; revised manuscript received 6 October 2008; published 30 October 2008)

In this paper, we use a set of rate equations to describe the thermal activation of a tip moving along a one-dimensional lattice, including the possibility of multiple back and forth jumps between neighboring potential wells. This description of an atomic-scale friction experiment is used to investigate how temperature acts as a lubricant, an effect that we refer to as *thermolubricity*. We discuss the detailed theoretical aspects of the model, which explains many aspects of the variation in atomic friction over a wide range of temperatures, velocities, and surface corrugations. We conclude that friction at low velocities and low surface corrugations is much lower than the weak logarithmic velocity dependence predicted before. Another consequence of the model is the trivial result that friction is zero in the zero-velocity limit. We confront numerical results from our theoretical model with experiments, in which the surface corrugation was controlled by use of geometrical effects, to demonstrate the experimental existence of thermolubricity. Although the calculations produce excellent fits to our data, the values of the fitting parameters clearly indicate that the underlying single-spring model suffers from an intrinsic flaw, which we ascribe to either the absence of flexibility of the tip or the restriction to a one-dimensional sliding geometry.

DOI: 10.1103/PhysRevB.78.155440 PACS number(s): 68.35.Af, 07.79.−v, 46.55.+d

I. INTRODUCTION

A. General

The role of temperature in atomic-scale friction recently has become a subject of deep interest in the field of nanotribology. As early as in 1928, Prandtl[1] recognized the effect of temperature and the reduction in friction due to thermal activation of macroscopic sliding objects. Although Prandtl[1] considered friction in a rather generic context, not describing the nanoscale details of the phenomenon, the results of his model capture the essence of the lubricating role played by temperature.

It has taken seven decades to demonstrate the importance of Prandtl's predictions[1] because, with the advent of the atomic force microscope (AFM) and especially the friction force microscope (FFM), it has become possible only recently to investigate these thermal effects experimentally on the atomic scale. Measurements on this scale can be performed with an atomically sharp AFM or FFM tip that is dragged over a crystal lattice under a modest normal load. The tip is connected via a flexible cantilever with a well-defined lateral spring constant k to a rigid support.

If we start by neglecting the role of thermal excitations, we can describe the motion of the tip within the framework of the Tomlinson model.[2] In the absence of thermal excitations, the only force available to make the tip overcome the atomic potential barriers is the spring force exerted by the support via the cantilever. That is, the tip mechanically slips to the next potential minimum when the combined system of the cantilever and the tip-surface interaction becomes unstable, which is the case when the tip is at a location where the second derivative of the surface potential U with respect to the tip position x is equal to the spring constant of the cantilever (i.e., $d^2U/dx^2=k$). As the consequence of this dragging, the tip repeatedly slips over the atomic barriers with a saw-tooth-like variation in the lateral force, which is known as stick-slip motion.

There are two important implicit assumptions within the Tomlinson model.[2] First, the tip resides always in a (local) minimum of the total potential (tip-surface interaction potential plus elastic energy of the deformed cantilever). Second, in every slip event the tip dissipates its excess energy instantaneously and completely, i.e., the motion of the tip in the local potential-energy well is overdamped. The landscape of local minima and maxima in the combined potential experienced by the tip changes continually with the motion of the support, new local minima being formed and existing ones being removed every time the support is moved over one lattice spacing of the substrate. When the depth of the local minimum in which the tip resides is reduced to zero the tip slips to the next minimum. We refer to these unstable points where the tip has to slip to the next potential minimum as *critical points*. At zero absolute temperature, the stick-slip motion of the tip faithfully reproduces the lattice of these critical points, which has precisely the same symmetry and lattice constants as the substrate lattice.

Thermal excitations assist the tip in overcoming the barriers prior to the critical points mentioned above. This introduces a stochastic element (noise) in the motion and reduces the average lateral force, i.e., leads to less friction. In this paper, we introduce thermal excitations in the Tomlinson model[2] and cast its solution in the form of a set of rate equations that we solve numerically. We end the paper by demonstrating these thermal effects in actual measurements of nanoscale friction on a graphite surface.

B. Modest thermal effects: The "thermal Tomlinson model (Ref. 2)"

As described above, the traditional Tomlinson model[2] describes friction on a very simple level. It involves only two contributions to the total potential energy of the system, namely, the energy stored in the cantilever spring and the tip-substrate interaction, and it provides a fully deterministic

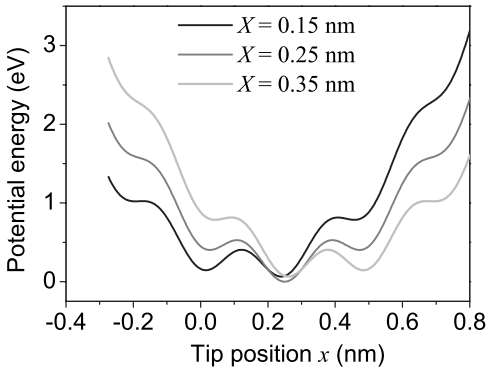

FIG. 1. Profiles of the combined potential of the cantilever spring and the interaction between the FFM tip and the surface, plotted as a function of the tip position x, as the support is dragging the tip along the X axis. The curves are for three different support positions X and have been calculated for a lateral cantilever spring coefficient of $k=1.8$ N/m and for a corrugation of the surface potential of 0.5 eV.

description of the atomic-scale stick-slip motion of the tip. We now first consider the effect of modest thermal vibrations of the atoms in the tip and those in the substrate. We start with the tip in one of the local minima in the combined potential, sketched in Fig. 1. Like all degrees of freedom of the cantilever-tip-substrate system, the vibrational mode connecting the present tip configuration with the next potential-energy minimum carries an average energy of $\frac{1}{2}k_BT$. When the support is translated parallel to the surface, the potential barrier height U separating the local minimum in which the tip resides from the next minimum gradually decreases. When it is comparable to a few times the thermal energy the tip has a high probability per unit of time to jump to the next potential minimum. In this way, at finite temperatures (and finite scan velocities) the tip almost never reaches the critical point at which the system is mechanically unstable and the tip is forced to slip. The role of thermal activation manifests itself in any time dependent experiment on atomic friction. The simplest example is the velocity dependence. Glosli and McClelland[3] were the first who examined this in atomic friction using molecular-dynamics simulations. They investigated the rupture of molecular bonds and the resulting stick-slip motion of an AFM tip on polymers and modeled it on the basis of thermally activated motion of the tip between surface-potential wells. Using straightforward transition-state theory, they introduced an attempt frequency r_0 and a Boltzmann factor to predict the rate of successful forward jumps between neighboring potential wells in order to compute the flow of probability from one potential well to the next,[4,5]

$$\frac{dP(t)}{dt} = r_0 P(t) \exp\left(-\frac{\Delta U^+(t)}{k_B T}\right). \tag{1}$$

Here, $P(t)$ is the probability of finding the tip in a particular potential well and $U^+(t)$ is the height of the potential barrier remaining in the forward direction. The main assumption here is that the tip can perform a precritical jump to the next potential well, but the possibility of a reverse jump is completely neglected since the barrier height for such a reverse jump is much higher than the forward barrier. This simple picture predicts that one can vary the strength of the effect of thermal excitations on the sliding motion by varying either the temperature T, the amplitude U_0 of the corrugation of the tip-surface interaction potential, or the scan velocity V of the support. The dependence of the resulting friction force F_{fric} on T and on U_0 should be strong, while the dependence on V may be expected to show a weak logarithmic-type character in view of the exponential form of the Boltzmann factor.[4–8]

This activated process can be formulated in terms of the Fokker-Planck equation.[9] Dudko *et al.*[10] proposed an elegant treatment of the thermal activation of the tip, generalizing the Tomlinson model[2] by adding a noise term. Their model takes into account the irregular motion of the tip, as the temperature increases. This model only includes the effect of forward jumps and they argued that the inclusion of backward jumps would lead to a further reduction in friction at low velocities when the frequency of such jumps would be substantial. Dudko *et al.*[10] concluded that at lower velocities, atomic friction has a weak logarithmic dependence on the scanning velocity due to thermal fluctuations, while at higher velocities, viscous drag dominates.

C. Strong thermal effects: "Thermolubricity"

Recently, Evstigneev and Reimann[11] analyzed the thermal activation of the tip, for a wide range of spring constants, describing the rates of multiple back and forth jumps of the tip. Thermal excitations can result in multiple jumps of the tip, both in the direction of the moving support and against that direction. This implies that the logarithmic velocity dependence of atomic friction, which is the result of only the forward jumps, should be restricted to a limited velocity range.

Interestingly, comparatively little attention has been paid to the regime of low velocities, where thermal effects should manifest themselves at full strength.[12] An alternative way to view the tip motion under these conditions is as a form of "driven diffusion" or biased thermal drift. As we shall see, the contribution of reverse jumps depends strongly on T, U_0, and V and becomes significant when k_BT/U_0 is sufficiently high and/or V is sufficiently low. When the time that the support takes to travel over one atomic distance is long enough that the tip makes several spontaneous forward and reverse jumps in that time, the required bias to make the tip follow the slow support motion, i.e., to make the frequency of forward jumps slightly higher than that of reverse jumps, is very small; in other words the friction force becomes extremely low. For this situation we have introduced the term thermolubricity.[12]

In Secs. II and III we employ a set of rate equations that we evaluate numerically to analyze this low-velocity regime and its connection to the regime of intermediate velocities, where stick-slip motion is retrieved, with the logarithmiclike velocity dependence. We confront our model with published[13] as well as different experimental data, demonstrating clear thermal effects at different surface corrugations, and we report strong manifestations of thermolubricity in velocity-dependent atomic-scale friction measurements.

The model is able to produce an excellent fit to each data set. However, the value of one of the essential fitting parameters needs to be chosen very differently for each choice of the sliding velocity. This serves as a strong indication that our model is still incomplete. We propose that the missing element is either in the neglect of the high-frequency tip apex fluctuations that we have discussed in several recent publications about the two-mass-two-spring model for the dynamics of the friction force microscope[14–16] or in the one-dimensional geometry of the model.

II. MODEL

A. Basic parameters and possible regimes

The Tomlinson model[2] accounts for two contributions to the potential energy of the system, namely, the elastic energy of the cantilever and the interaction between the tip and the surface,

$$U(X,x) = \frac{U_0}{2}\left[1 - \cos\left(\frac{2\pi x}{a}\right)\right] + \frac{1}{2}k(X-x)^2, \qquad (2)$$

where a is the lattice constant of the substrate, x the position of the tip, and X the position of the support, which drags the tip over the potential barriers. Typical examples of this potential profile are given in Fig. 1. We define a dimensionless parameter, which we will refer to as the relative corrugation or the Tomlinson parameter,[2]

$$\gamma = 2\pi^2 \frac{U_0}{ka^2}. \qquad (3)$$

This parameter describes the relative strength of the potential corrugation with respect to the cantilever stiffness.

When $\gamma > 1$ the total potential energy of Eq. (2) exhibits several local minima, which leads to the familiar stick-slip instabilities in the motion of the tip. When $\gamma \leq 1$, i.e., when the cantilever is sufficiently stiff with respect to the surface corrugation, there is only a single stable minimum in the total potential energy for every support position. Under these conditions, the cantilever distortions (compression and elongation) still follow the sinusoidal atomic corrugation of the surface, but the motion is smooth and exhibits no stick-slip instabilities. Within the Tomlinson model,[2] the net friction force is zero in this case, the backward lateral forces experienced while climbing the potential hills being precisely equal to the forward forces felt half a period later while descending into the valleys. In other words, the energy invested in the first half of the period is returned to the system during the second half, as a result of which there is no energy dissipation. There are several ways to bring a sliding system into this regime. Socoliuc *et al.*[17] reduced the amplitude U_0 of the tip-surface potential by scanning their tip over an NaCl(100) surface at significant negative normal forces, i.e., while pulling against the van der Waals attraction between tip and surface, until they found reversible sliding with ultralow dissipation. Dienwiebel *et al.*[13] measured the lateral forces between a graphite flake and a graphite surface. By rotating the two lattices with respect to each other, they were able to make U_0 low enough to result in ultralow dissipation, even for substantial (positive) normal forces. In this case, where the slipperiness is caused by the incommensurability of the contacting lattices, we speak of *superlubricity*.[13,18–20] We should realize that in the cases of ultralow friction discussed here, the dissipation is not completely absent. Even when stick-slip instabilities are completely avoided, the system can lose energy irretrievably by processes such as electron-hole pair generation.

We return to the stick-slip case, where $\gamma > 1$. It is easy to derive the values of γ at which the number of local minima in the potential changes. For instance, if $1 < \gamma < \frac{3}{2}\pi$, the total potential U will have either one or two wells, depending on the position X of the support. Generally, there will be n or $(n-1)$ wells when $\frac{2n-3}{2}\pi < \gamma \leq \frac{2n-1}{2}\pi$.

At nonzero temperature the dynamics of the tip are to be taken into account. There are four basic time scales or frequencies involved in this problem: (1) the frequency with which the support scans over the atomic lattice; (2) the frequency ν of rapid inherent motion of the tip-cantilever combination in a potential well, which depends weakly on the tip position, $\nu = (2\pi)^{-1}M^{-1/2}(k + 2\pi^2 U_0/a^2)^{1/2}$, with M as the effective mass of the cantilever-plus tip; (3) the frequency of successful thermally activated jumps between potential wells; and (4) the damping parameter η, which is the rate of relaxation of the energy and momentum of the tip-cantilever combination into the phonon bath and into other excitations of the substrate, tip, or cantilever.

We assume the backward and forward jump rates $r_i^{\pm}$ of the tip between neighboring potential wells to follow a simple Arrhenius law,

$$r_i^{\pm} = r_0 \exp\left(-\frac{U_i^{\pm}}{k_B T}\right), \qquad (4)$$

where the subscript i refers to the specific potential well, $U_i^{\pm}$ is the potential-energy barrier for a forward jump (+) to well $i+1$ or for a reverse jump (−) to well $i-1$, and the pre-exponential factor r_0 is the attempt rate for such jumps. Since the potential profile within the Tomlinson model[2] itself is changing continually due to the support motion, the potential barriers are functions of the support position, i.e., $U_i^{\pm} = U_i^{\pm}(X)$. We follow the simple form of transition-state theory and equate the pre-exponential factor r_0 of Eq. (4) to the vibrational frequency ν.

Equation (4) explicitly shows us that when the support moves forward and reduces the forward energy barrier, the rate of jumps to the next local energy minimum increases exponentially (Fig. 2). This makes the precritical jumps almost inevitable while jumps from deep potential wells can be rather infrequent.

At this stage, we introduce two dimensionless parameters that allow us to distinguish between several qualitatively different friction regimes,

$$\alpha \equiv \frac{V}{a\nu} \approx \frac{V}{a\eta},$$

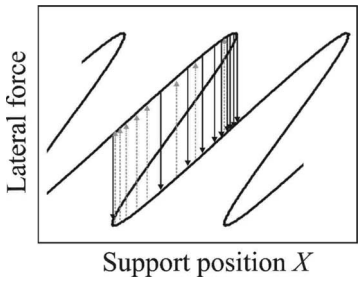

FIG. 2. Variation in the lateral force with the support position X [solutions of Eq. (2)]. The exponentially varying probabilities of thermally assisted jumps are indicated here via the density of solid arrows (forward jumps) and dashed arrows (backward jumps).

$$\beta \equiv \left(\frac{V}{a\nu}\right)\exp\left(\frac{U_0}{k_B T}\right) = \alpha \exp\left(\frac{U_0}{k_B T}\right). \tag{5}$$

Here, α shows how fast or slow the scanning process is with respect to both the inherent motion of the tip in a surface-potential well and the relaxation rate of the momentum to the thermal bath; β is a parameter that shows how fast or slow the scanning process is with respect to the rate of activated jumps of the tip between neighboring surface-potential wells. Obviously, the two parameters are related.

Stick-slip motion occurs in the velocity regime, where the support drags the tip to the next minimum before the tip jumps by itself due to thermal activation. In terms of the two parameters, this implies that the stick-slip regime corresponds to the case $\alpha \ll 1$, $\beta \gg 1$, where thermal activation is negligible and the tip *sticks* nearly everywhere in a potential well except in the vicinity of the critical point where it will make a precritical jump to the next well. There are two important time scales involved in this process: one is the slow time variation in the support motion that drags the tip to the next potential well and the other is the rapid motion of the tip apex within each potential well. The first inequality $\alpha \ll 1$ assures that the movement of the tip from the critical point to the neighboring well is much faster (actually on the order of ν^{-1}) than the slower motion of the support. So it is seen by the support as a fast *slip*. The excess energy released during the transition from the critical point to the bottom of the well is completely dissipated in the slip event (on a time scale of η^{-1}). This is the origin of the fact that the friction force in this regime is independent of the characteristic dissipation rate. The slip starts in the vicinity, but, due to thermal excitations, just before the critical point, which leads to a logarithmic velocity dependence of the friction, as mentioned before.[4,5] Thermal activation of the tip manifests itself much more strongly when we reduce β, which can be accomplished not only by lowering the velocity but, equivalently, also by increasing the temperature or reducing the amplitude of the potential. When $\beta \ll 1$, the scanning is slow with respect to the natural occurrence of thermally activated jumps between neighboring surface-potential wells. In this regime, the tip can be found on average at a position $\bar{x}$ that effectively "drifts" with the support position X, while the average difference $X-\bar{x}$ determines the mean lateral force. Although the instantaneous lateral force exhibits rapid irregular fluctuations with an amplitude in the order of the maximum possible tip-surface force, the average lateral force is significantly lower. We call this range of low velocities the *thermal drift* regime. In the intermediate situation, say at $\beta \simeq 1$, the tip exhibits on average one random jump per lattice spacing traveled by the support. In this case, we expect to observe irregular or stochastic stick-slip motion.

B. From stick slip to thermal drift

1. General approach

Here we concentrate on the cases $\alpha \ll 1$, $\beta > 1$, and $\beta < 1$, which cover both the stick-slip and thermal drift regimes. The average behavior of the system can be described by an appropriate kinetic equation for the distribution function (probability density) to find the tip at a certain time at a certain position x. In the case $\alpha \ll 1$ under consideration, this complicated situation can be substantially simplified by the fact that, while being in a certain potential well, the motion of the tip both in physical space and in energy space (characterized by ν and η, respectively) is fast with respect to the velocity of scanning.

The most dominant time scales at play in the measurements are the long time scale of the slow scan motion and the short time scale of the rapid motion of the tip within the potential wells. In view of the large difference between these time scales, we can average over the faster class of processes and replace the probability density $p(x,t)$ by a discrete set of probabilities $p_i(t)$ of finding the tip in well i at time t. Assuming that the transitions between neighboring wells follow the Arrhenius law described by Eq. (4), we formulate the rate of change in the probability $p_i(t)$ to find the tip in well i in terms of the jump rates between well i and the two neighboring wells, $(i-1)$ and $(i+1)$. In this way, the kinetic equation is reduced to a system of continuity equations for $p_i(t)$ in discrete space of the form

$$V\frac{dp_i}{dX} = \frac{dp_i}{dt} = -(r_i^+ + r_i^-)p_i + r_{i-1}^+ p_{i-1} + r_{i+1}^- p_{i+1}. \tag{6}$$

Again, V is the scan velocity, with which the support moves over the surface, and p_i, p_{i-1}, and p_{i+1} are the probabilities of finding the tip in wells i, $i-1$, and $i+1$. The jump rates $r_i^{\pm}$ are determined by Eq. (4), with the potential barriers $U_i^{\pm}(X)$ for forward or backward jumps from well i depending on support position X. This set of differential equations naturally describes all regimes involving thermal activation of the tip. At low surface corrugations it incorporates the effects of multiple back and forth jumps between neighboring potential minima and at higher surface corrugations it describes the flow of probability when the tip motion reduces to the familiar precritical jumps that take place when the remaining forward barrier $U_i^{\pm}(X)$ is a few times the thermal energy $k_B T$ or lower.

The mean (ensemble-averaged) lateral force as a function of the support position X can be found as $\bar{F}(X) = -k(\bar{x}-X)$. The mean position of the tip, which appears in this expression, is given by $\bar{x} = \bar{x}(X) = \Sigma p_i(X) x_{\min}^{(i)}(X)$. Here, the $x_{\min}^{(i)}$ represent the X-dependent positions of the wells (i.e., all local minima of the total potential).

Let us consider a simple situation in which at most two local minima exist in the total potential energy. Since the total probability is 1 and hence $p_1+p_2=1$, the system of Eq. (6) is reduced to a unique equation for, say, p_1 (the probability to be in the left well). Moreover, it is sufficient to find a solution only for the motion over one period of the surface potential, say, $0<X<a$. This is allowed by the fact that the coordinate of the critical points corresponding to the disappearance of the well of origin is smaller than a. Furthermore, nontrivial behavior takes place only in the interval between the critical points X', where a new well appears, and X'', at which the previous well disappears. Outside of this interval either $p_1=1$ (for $0<X<X'$) or $p_1=0$ (for $X''<X<a$). In the interval of interest $X'<X<X''$, the equation for p_1 takes the form

$$V\frac{dp_1}{dX} = -r_1^+ p_1 + r_2^-(1-p_1), \tag{7}$$

with $r_1^+=\nu\exp(-U_1/k_BT)$ and $r_2^-=\nu\exp(-U_2/k_BT)$. Here U_1 and U_2 are the barriers between the two minima as seen from the left and the right, respectively. Note that, for the given potential of the form of Eq. (2), these quantities are known, albeit cumbersome functions of X. The mean (ensemble-averaged) lateral force as a function of X is given by

$$\bar{F} = -k[p_1 x_{\min}^{(1)} + (1-p_1)x_{\min}^{(2)} - X]. \tag{8}$$

2. Zero limit of β: The limiting case of zero velocity

We stay with the simple case, where only two potential-energy wells exist. In the limit of vanishingly small β, we neglect the term in the left-hand side of Eq. (7) and find

$$p_1^{(0)} = \frac{r_2^-}{r_1^+ + r_2^-}. \tag{9}$$

Physically, this expression, together with $p_2^{(0)}=1-p_1^{(0)}$, describes the equilibrium distribution of positions of the tip established in the situation when activated jumps between the wells have enough time to occur many times before a sizable displacement of the support takes place.

Since the ensemble-averaged lateral force $\bar{F}^{(0)}(X)$ at position X is periodic with the lattice constant a, averaging over one lattice spacing gives us the mean value of the lateral force—the friction force—on a large time scale. An immediate result is that the friction force in the zero limit of β is zero, i.e.,

$$F_{\text{fric}}^{(0)} = \frac{1}{a}\int_0^a \bar{F}^{(0)}dX = 0. \tag{10}$$

Since $\beta\propto V$, we conclude that

$$\lim_{V\to 0} F_{\text{fric}} = 0. \tag{11}$$

We see that the friction force at finite temperature should vanish in the zero-velocity limit because of the thermally activated jumps of the tip between the surface-potential wells. For any given surface corrugation and any nonzero temperature, thermal jumps occur and, due to the thermal drift motion described here, friction will vanish in the limit of zero velocity.

In a sense, the result of Eq. (11) is trivial. In fact, speculations have been published that friction might vanish as the velocity goes to zero.[10] However, in many studies, this possibility has been ignored or overlooked. There is even a study, performed with the extended adiabatic approximation method, which suggested that whenever the thermal energy would be lower than the potential barrier, static friction would not vanish, even in the zero-velocity limit.[21]

This result is important in at least two respects. First, a strong decrease in the friction force with decreasing velocity is expected when going down in velocity from the stick-slip regime to the deep thermal drift regime, where F_{fric} becomes small and finally vanishes when $V\to 0$. The overall behavior for any given relative corrugation can be obtained from a numerical solution of the corresponding system of equations [Eq. (6)].

Second, the role of thermally activated processes requires us to reconsider static friction. Static friction is the minimum force required to set an object at rest into motion along the surface. Within the classical Tomlinson model,[2] this force is given by the maximum value of the lateral surface force, which is determined by the corrugation of the surface potential, $F_{\text{static}}=\pi U_0/a$, and it is independent of whether the subsequent motion is dissipative ($\gamma>1$, $F_{\text{fric}}=F_{\text{fric}}(U_0,\gamma)\neq 0$) or nondissipative ($\gamma<1$, $F_{\text{fric}}=0$). Apparently, the usual definition of static friction tacitly implies observation on a sufficiently short time scale that thermal effects can be ignored. On a larger time scale the object will exhibit thermally activated motion. In the absence of an external force, this is a random walk along the surface, while in the case of a slowly increasing bias the walk is not random but has the character of biased diffusion. In this case, the system is not static and the definition of static friction loses its meaning. The static friction force could be understood as an essentially conditional quantity. It is given by the maximum surface force, provided that the external force increases sufficiently rapidly and it will be smaller for a more slowly ramped external force, as a result of the thermal jumps. Static friction will simply vanish if the external force is ramped up sufficiently slowly.

3. First-order approximation in β: Friction in the thermal drift regime

In Eq. (6), if we introduce a first-order order term $p_1^{(1)}\sim\beta$ in the probability $p_1\equiv p_1^{(0)}+p_1^{(1)}$ for the tip to reside in the first well and neglect second-order terms in β, we get

$$p_1^{(1)} = -V[r_1^+ + r_2^-]^{-1}\frac{dp_1^{(0)}}{dX}. \tag{12}$$

Substituting this in Eq. (7) for the evolution of the probabilities in the two-well case, we obtain

$$p_1^{(1)} = -Vr_1^+ r_2^-[r_1^+ + r_2^-]^{-3}\left[\frac{1}{k_BT}\frac{dU_2}{dX} - \frac{1}{k_BT}\frac{dU_1}{dX} + \frac{1}{\nu_1}\frac{d\nu_1}{dX} - \frac{1}{\nu_2}\frac{d\nu_2}{dX}\right]. \tag{13}$$

We have introduced the last two terms to take into account

explicitly that the attempt frequencies ν_1 and ν_2 for forward and reverse jumps between wells 1 and 2 can be different from each other and dependent on support position X, for example, by making them proportional to the square root of the curvature of the local potential. Note that $p_2^{(1)}=-p_1^{(1)}$. Here, $p_1^{(1)}$ and $p_2^{(1)}$ describe the nonequilibrium correction to the distribution of tip positions due to the fact that at nonzero scanning velocity thermally activated jumps do not have enough time to establish the true equilibrium distribution at each support position X. As seen in Eq. (12), the effect is proportional to two factors: the first factor, $V[r_1^+ + r_2^-]^{-1}$, shows how large is the systematic lack of time required to realize the changes needed at every new support position X and the second factor, $dp_1^{(0)}/dX$, shows how $p_1^{(0)}$ changes with X, i.e., what changes in the distribution are to be realized by the jumps. If the system moves to the right ($V>0$), these changes are due to the first well becoming more shallow and the second well becoming deeper. As seen from Eq. (13), all four contributions to $p_1^{(0)}$ are positive. Consequently, the overall effect is seen as a systematic delay of the transfer of the tip from the first to the second well. Clearly, on average, this will lead to an increase in the ensemble-averaged lateral force. The friction force experienced by the tip at nonzero velocity will be nonzero.

Indeed, calculating the ensemble-averaged lateral force as in Eq. (8) with $p_1=p_1^{(0)}+p_1^{(1)}$ using Eqs. (8) and (13) we see that $\bar{F}(X)$ is larger than $\bar{F}^{(0)}(X)$ at every support position X (except for the intervals where they coincide due to the temporary absence of a second potential well). Averaging $\bar{F}(X)$ over one lattice spacing,

$$F_{\text{fric}} = \frac{1}{a}\int_0^a \bar{F} dX, \tag{14}$$

we obtain the friction force, which is nonzero at nonzero velocity.

Now we assume for simplicity that, except at very high temperatures, the effect of changes in the vibrational frequencies ν_1 and ν_2 with changing X can be neglected with respect to the more pronounced effect of changes in the potential barriers, i.e., we neglect the last two terms in Eq. (13). This leads to the following approximation to the average lateral force:

$$F_{\text{fric}}|_{\beta\ll 1} \approx \frac{Cka}{4}\frac{U_0}{k_BT}\beta = \frac{CkV}{4\nu}\frac{U_0}{k_BT}\exp\left(\frac{U_0}{k_BT}\right). \tag{15}$$

Here, ν and U_0 are the characteristic values of the vibrational frequency and the barriers in the total potential, respectively. C is a dimensionless quantity representing the relative width of the region of the support positions for which there is more than one well in the total potential as a function of the tip position, and hence, thermally activated jumps can occur. It varies between $C=0$ at $\gamma=1$ and $C\approx 1$ at $\gamma=3\pi/2$. The friction force vanishes at $\gamma\leq 1$, as a reminiscence of the classical Tomlinson model.[2]

In the thermal drift regime, where $\beta\ll 1$, Eq. (15) gives the friction force linear in the scanning velocity, and it strongly—exponentially—depends on both the effective corrugation and the temperature. Even a small decrease in U or a small increase in T can lead to a substantial reduction in friction. By initiating motion of the tip, here, temperature acts as a *lubricant*.

In the derivations above, we assumed for simplicity that the rates of thermally activated jumps of the tip can be calculated in the framework of transition-state theory, so that the pre-exponential factors were taken simply to be the vibrational frequencies, $r_0=\nu$. This traditional approximation tacitly assumes that the damping coefficient in the equation of motion is of the order of the vibrational frequency, $\eta\sim\nu$. A more general approach, valid for the case of both moderate and strong dampings, allows estimating the jump rate prefactor as $r_0=\nu^2/\eta$. For this case, after revision of the derivations given above, the result [Eq. (15)], with a modest redefinition of the γ-dependent dimensionless factor C, becomes

$$F_{\text{fric}}|_{\beta\ll 1} \approx C^*\frac{U}{k_BT}\exp\left(\frac{U}{k_BT}\right)\eta MV, \tag{16}$$

with M as the effective mass. This result is instructive in several respects. First, we have an apparent result that the friction force is proportional to the damping coefficient η. With increasing damping, at any surface corrugation, thermal jumps become rarer and their role as a lubricant therefore reduces, thus increasing friction toward the much higher value characteristic for stick-slip type of motion.

Second, we notice that ηMV is equal to the friction experienced by an object of mass M moving along a featureless surface with constant velocity V, as a result of dissipation to the thermal bath with rate η. Thus we expect friction to approach $F_{\text{fric}}=\eta MV$ at very high V. The lower-velocity friction reflects the nontrivial physics behind the thermal drift motion of the tip. If the thermal jumps had enough time to establish the equilibrium distribution of the tip positions around the support position, the (mean) friction force would be close to ηMV, as a result of the motion with mean velocity of the order of V. However, due to the lack of time at any nonzero velocity, the distribution is not in equilibrium. A systematic delay of the tip with respect to the mean equilibrium position, as discussed above, manifests itself as an increase in friction. This effect is stronger when the jumps become less frequent, i.e., at larger U/T, as seen from Eq. (16). It is to be noted that the friction forces, although larger than ηMV, remain significantly lower than the value $\sim U_0/a\sim ka$ characteristic for the stick-slip motion, which takes place when thermal jumps can be neglected.

4. Velocity dependence of friction over the full range of V

We briefly summarize the results from our model. In the limiting case of large velocities ($a\gg 1$), the surface corrugation does not perturb the motion of the tip, which follows the support with constant velocity V. Friction is due to the direct dissipation to the substrate (interaction with the phonon bath) and hence it is linear in V, $F_{\text{fric}}=\eta MV$.

At lower velocities ($a\ll 1$ and $\beta\gg 1$) the surface corrugation forces the tip to perform quasiregular stick-slip motion. To restore motion of the tip after every stick event, an external force is required in the order of the maximum surface

force, so that $F_{\text{fric}} \sim U_0/a$ (which is $\sim ka$ when γ is not too large). The weak velocity dependence of friction in this regime is mainly caused by thermally activated jumps in the vicinity of the critical support positions, where the potential barrier becomes small.

At even lower velocities ($\beta \ll 1$), thermally activated jumps of the tip ruin the quasiregular stick-slip motion and change it into a stochastic thermal drift. The friction force is much lower than in the stick-slip case, being now caused by a small deviation of the average position of the (strongly fluctuating) tip from the support position. On the other hand, the friction force turns out to be larger than it would be in the case of constant velocity, since an effect of surface corrugation is still there, although it now comes in a different way than in the stick-slip regime.

In the limiting case of zero velocity, the friction force vanishes since in this case, thermally activated jumps ruin any effect of surface corrugation in the motion of the tip on average. The thermal drift regime appears at low scanning velocities, at elevated temperatures, or at lower surface corrugations. In view of the strong exponential dependence of β on U/T, the transition between regimes can take place due to even a small change in temperature or surface corrugation. Interestingly, the effective corrugation of the tip-surface interaction can vary in a very wide range. In Sec. IV, we will mention in detail how these possibilities are realized.

III. NUMERICAL EVALUATION OF THE RATE EQUATION: COMPLETE SOLUTIONS

We can analyze Eq. (6) numerically without any simplifying approximation. To this end, we evaluate the probabilities at regular time intervals $\Delta t = \Delta X/V$, where ΔX is a small step in support position (typically 0.001 nm) and V is the constant scan velocity of the support. Assuming that at $X = 0$, the probability of finding the tip in the first well is unity, the probabilities are evaluated using the values of the potential barriers corresponding to each discrete position of the support position. For each interval ΔX, the change in probability Δp_i is estimated in each well, and the calculation is performed over a total of four lattice spacings or more, i.e., for X ranging from zero to $4a$ or higher. We check that the results over the last lattice spacing are identical to those one lattice spacing earlier, thus ensuring that the results are not affected by the initial condition that $p_i(X=0)=1$. For each of the support positions $X_n (n=1,2,\ldots,N)$ over the fourth lattice spacing we calculate the average tip position. With the average tip position, the average lateral force $\bar{F}(X_n)$ at each position X_n or time X_n/V is then calculated. The friction force is obtained by averaging this over the fourth lattice spacing,

$$F_{\text{fric}} = \frac{1}{N}\sum_{n=1}^{N} \bar{F}(X_n). \tag{17}$$

In Fig. 3 we have plotted examples of the evolving probabilities in each well, for two relative surface corrugations of $\gamma=8$ and $\gamma=3$, a cantilever spring constant of $k=1.8$ N/m and a support velocity of $V=30$ nm/s. At the higher corrugation [Fig. 3(a)] either two or three wells are present in the potential, depending on the support position X. We see that the probability to find the tip in the initial potential well reduces smoothly to zero while the probability of finding it in the second well approaches unity. This high corrugation has situated the system in the regime of precritical jumps, in which backward jumps are very infrequent. At the lower relative corrugation [Fig. 3(b)] only one or two wells are

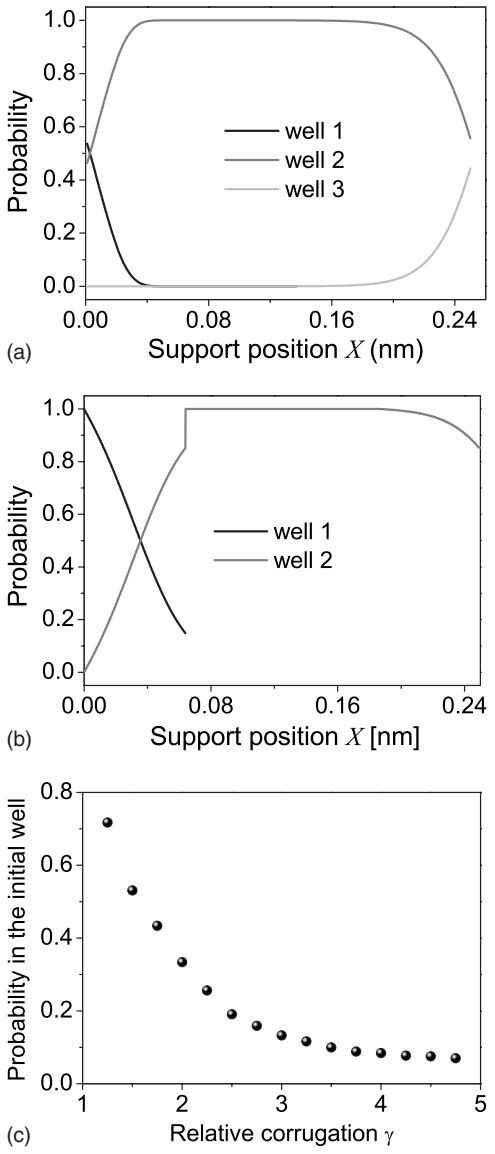

FIG. 3. Evolution of the probabilities to find the tip in the local wells of the total potential-energy profile calculated for a cantilever spring constant of 1.8 N/m, an attempt frequency of 1.6 kHz, and a support velocity of 30 nm/s. (a) At a high relative surface corrugation of $\gamma=8$ precritical jumps dominate. They make the probability in the initial well reduce smoothly to zero before the Tomlinson instability point (Ref. 2) is reached and the initial well disappears. Under these conditions the rate of backward jumps is negligible. (b) At a low relative surface corrugation of $\gamma=3$ forward and backward jumps are frequent also when the system is not close to a critical point. The tip has a significant probability to be in the initial well even at the support position at which this well disappears, as is plotted in panel (c).

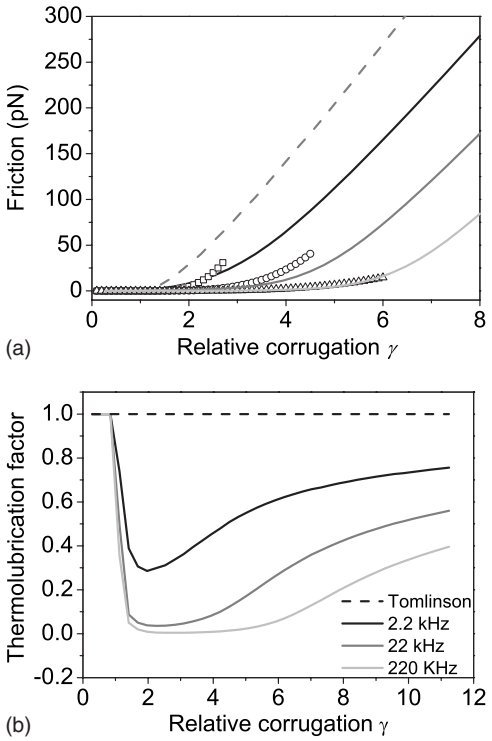

FIG. 4. (a) Friction as a function of the relative corrugation γ, predicted by the Tomlinson model (Ref. 2) (dashed curve) and by the thermolubricity model (symbols and solid curves). The calculations were performed for a lattice constant of 0.246 nm, a spring constant of 1.8 N/m, and a support velocity of 30 nm/s to compare with experimental data. These calculations illustrate the dramatic suppression of friction for different values of the attempt frequency of ν=2.2 kHz (black curve and squares), 22 kHz (dark gray curve and circles), and 220 kHz (light gray curve and triangles). The solid curves show the results of the numerical calculations and the symbols give the analytical results of the first-order approximation in β. When the attempt frequency is high enough, friction can be very low even at relatively high corrugations. (b) Ratio of the friction values predicted by the thermolubricity model to corresponding values from the Tomlinson model (Ref. 2), plotted against the relative corrugation γ. We refer to this ratio as the thermolubrication factor. The dashed horizontal line is the Tomlinson model itself (Ref. 2). The solid curves approach the Tomlinson line (Ref. 2) at high corrugations, where only precritical jumps occur.

present. The probability of finding the tip in the initial potential well remains well above zero all the way up to the point where the well disappears [Fig. 3(c)]. Under these conditions the rate of backward jumps is in the same order of magnitude as the rate of forward jumps and the tip jumps back and forth many times per lattice spacing traveled by the support.

Figure 4(a) combines the results of such calculations for a large number of relative corrugations γ, for the 0.246 nm lattice constant of the graphite basal plane, an effective cantilever spring constant of 1.8 N/m estimated from the friction experiments, a velocity of 30 nm/s, and for three different values of the attempt frequency ν in the form of a plot of the friction force versus γ. The plot shows that the Tomlinson model[2] predicts dissipationless sliding of the tip for relative corrugations $\gamma \leq 1$. In the case of weak thermal effects, i.e., when only precritical jumps occur, and the friction force develops a weak logarithmic velocity dependence, Eq. (1) predicts a modest lowering of the friction force with respect to the Tomlinson curve.[2] The lower three curves in Fig. 4(a) show the numerical results for the case of strong thermal effects. In that case, significant lowering of the friction force is possible even at relative corrugations much higher than 1. These results show that temperature can act as a very efficient lubricant.

A counterintuitive aspect of the calculations in Fig. 4(a) is that the difference with the Tomlinson curve[2] increases toward higher γ values, whereas one might expect that at higher corrugations the effect of thermal excitations should become less important. This seeming contradiction is resolved by looking at the relative values, as we have done in Fig. 4(b). We refer to the reduction factor between the thermally lowered friction force and the friction force expected within the Tomlinson model[2] as the "thermolubrication" factor. As Fig. 4(b) shows, this factor can be significantly below unity for an intermediate range of γ values where thermal effects manifest themselves very strongly via high frequencies of spontaneous forward and backward jumps, but at higher γ values it necessarily approaches unity when only precritical jumps remain in an ever narrower range of X positions before each critical point.

IV. EXPERIMENTS

A. Dependence of friction on potential corrugation

Two remarkable experiments reported recently have shown the reduction in friction by reducing the surface corrugation deliberately—one by varying the normal load exerted by the scanning tip on the surface[17] and the other by varying the relative orientation of the lattices of two surfaces that were sliding over each other.[13,22] In the first case, the normal load was controlled so that the relative potential corrugation γ was varied over a wide range, and when the normal load was reduced sufficiently that $\gamma \leq 1$, the system slid with nearly zero dissipation. In the latter case, a tungsten tip was scanning over a graphite surface, but a graphite flake was strongly attached to the tip, so that the sliding actually took place between two graphite lattices. By rotating the substrate around the tip axis the degree of (in)commensurability between the two lattices could be tuned. This made the potential corrugation maximal for a narrow region of flake-substrate orientations where the two lattices were in registry and could only slide with high dissipation, while it made the corrugation extremely low and leading to superlubricity for a wide range of nonmatching orientations.

For the latter experiments, we used a dedicated high-resolution friction force microscope, featuring a two-dimensionally sensitive cantilever—the Tribolever™—with equal lateral (X and Y) spring constants of 5.75 N/m. Combined with the lateral tip compliance, this resulted in an effective lateral spring constant of 1.8 N/m. The details of the instrument have been given elsewhere.[23,24] Here, we reanalyze the experimental data on superlubricity in Ref. 22, in search for thermal effects at a range of relative corrugations.

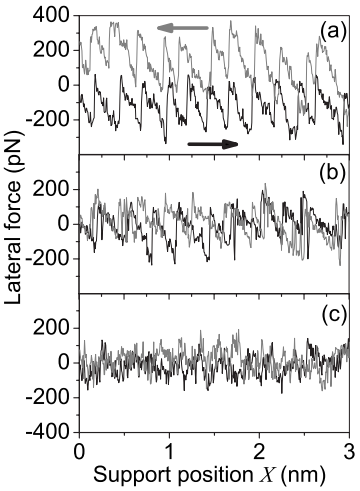

FIG. 5. Variation in stick-slip behavior between different rotation angles of a graphite flake with respect to a graphite substrate (data from Ref. 13). The black and gray curves are the forward and reverse scans. (a) At a relative orientation of 0° the lattices are in registry and dissipation is high. In this case we observe well-defined stick-slip motion. (b) At an intermediate orientation of 5° the system is partially out of registry and the stick-slip motion is irregular and we observe additional spontaneous backward and forward jumps. (c) At 20° the lattices are more incommensurate and it is difficult to recognize any stick-slip character in the stochastic motion of the tip. We use the Tomlinson model (Ref. 2) to estimate the potential corrugations from the friction loops using Eq. (19), from which we obtain the following estimates: (a) $\gamma=5.25$, (b) $\gamma=3.33$, and (c) $\gamma=2.47$. Note that even in panel (c) the system is not superlubric, i.e., $\gamma>1$.

The friction loops in this experiment clearly exhibit systematic changes in the motion of the tip, as sensed by the Tribolever. Figure 5 depicts typical friction loops observed under three different substrate-flake orientations, namely, (a) in registry, (b) partially out of registry, and (c) even more out of registry. The three force loops in Fig. 5 are all for γ values above unity. As γ is reduced, the area enclosed by the friction loop shrinks, i.e., the friction force is reduced. We recognize that also the nature of the friction loop changes from that of well-defined nearly regular stick-slip instabilities (a) to irregular stick slip with superimposed spontaneous backward and forward jumps and (b) to completely stochastic driftlike motion. This change in character indicates that in this experiment the reduction in the friction force is due to a large part to spontaneous thermal jumps.

For a full quantitative comparison between the experiment and our theory, we have made a careful selection of force loops. This was necessary because the actual motion of the tip (flake) is essentially two dimensions, whereas the theory has been restricted to a one-dimensional lattice. In the experiments in Ref. 22 a large part of the scans has been performed for a sliding direction parallel to the [0001] crystallographic axis of the graphite substrate. The fully two-dimensional sensitivity of the Tribolever allowed for measurements in which this alignment was maintained even when the tip and substrate were azimuthally rotated with respect to each other. In the two-dimensional force maps, in particular, those at higher friction forces (closer to commensurate contact), we could easily recognize a periodic pattern of scan lines exhibiting a single period of 0.246 nm, corresponding to nearly one-dimensional trajectories of the flake over the two-dimensional substrate, and scan lines with two periods of 0.246 and 0.142 nm, corresponding to more zigzag-type trajectories. Since the lattice period plays a key role in our theory, we have selected for our quantitative analysis the one-dimensional type scan lines (force loops) with a single lattice period. We have verified that without this selection procedure the outcome of our analysis is not significantly different.

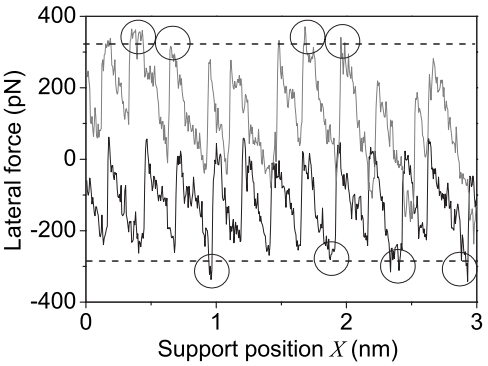

FIG. 6. Illustration of the selection of force maxima for the determination of γ. The average of the highest force maxima, encircled here, was used to obtain $F_{\max}$ from which γ was calculated using Eq. (19). The dashed lines indicate the values determined for the selected loop.

The relative corrugation γ can be estimated from the force variations in a friction loop by use of the Tomlinson model,[2] which relates the maximum force $F_{\max}$ to the amplitude of the potential U_0,

$$F_{\max}=\pi\frac{U_0}{a}. \tag{18}$$

Combining this expression with Eq. (3), we can readily estimate the relative corrugation γ completely in terms of experimental parameters, namely, the spring constant k, the lattice parameter a, and the maximum lateral force $F_{\max}$,

$$\gamma=2\pi\frac{F_{\max}}{ka}. \tag{19}$$

One of the effects of precritical jumps is to reduce the average maximum force with respect to the value from Eq. (18). However, if we concentrate on individual force maxima and select the highest ones, we hope that we can still obtain a relatively good albeit somewhat low estimate of $F_{\max}$. In practice we have used the average of a few of the highest force peaks in a set of friction loops to estimate $F_{\max}$ for each set of conditions. This procedure is illustrated in Fig. 6. Because the γ value obtained from this procedure is a lower estimate of the true γ in the experiment, we will further refer to it as the *apparent* γ.

The result of our analysis for the selected "one-dimensional" scan lines is plotted in Fig. 7 as the friction force against the (apparent) relative corrugation γ. Also

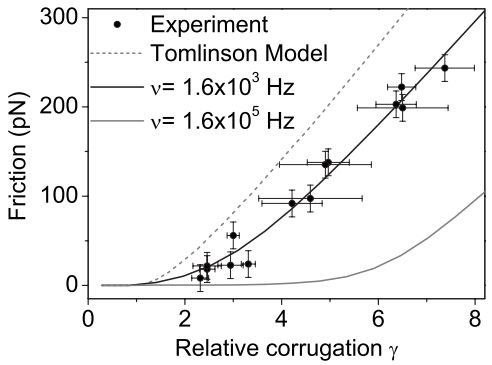

FIG. 7. Friction against relative corrugation. The data points are obtained from the experiment. They are compared with the prediction from the Tomlinson model (Ref. 2) (dashed curve) and results for the thermolubricity model (solid curves). The parameters used in the calculations are obtained from the experiment ($k=1.8$ N/m, $a=0.246$ nm, and $v=30$ nm/s). The thermolubricity model is shown here for two values of the attempt frequency. Excellent agreement is obtained with the experimental data for an attempt frequency of 1.6 kHz.

shown in Fig. 7 are friction forces calculated numerically for the parameter values of, characteristic for the experiment, $k=1.8$ N/m, $a=2.46$ nm, and $v=30$ nm/s. We immediately recognize that the experimental results are systematically below the curve calculated with the Tomlinson model.[2] Note that since the apparent γ's used for the experimental points in Fig. 7 are lower than the actual γ's, the difference between the measured friction curve and the Tomlinson curve[2] must be even larger than Fig. 7 suggests. The significant lowering of the friction force is a clear indication for the effect of thermal excitations in the motion of the tip. The thermal effects manifest themselves most strongly at lower relative corrugations, where they make friction nearly vanish well above $\gamma=1$.

The two lower calculated curves incorporate the effect of thermal jumps for two different values of the only fitting parameter in our model, which is the attempt frequency for thermally activated jumps, ν. As Fig. 7 shows, the fit of the model calculation to the experimental data is excellent for a value of $\nu=1.6$ kHz. This frequency is of the same order of magnitude as the resonance frequency of the Tribolever used, which suggests that the thermal vibrations of the entire cantilever dominate the thermolubricity effect. However, we will be confronted with evidence opposing this naive interpretation in Sec. IV B.

B. Dependence of friction on scan velocity

The average number of thermally activated jumps that the tip makes to a neighboring potential-energy minimum per lattice spacing traveled by the support ($\sim\beta^{-1}$) is proportional to the time required for the support to traverse one lattice spacing. Therefore, the velocity dependence of the friction force is a straightforward way to address the effect of thermal excitations. As we discussed in Sec. II B, friction should vanish in the zero-velocity limit and this should proceed much more dramatically than the weak logarithmic velocity dependence that has been predicted and found at higher velocities (Sec. I B).

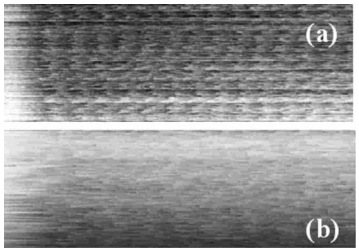

FIG. 8. Two lateral force images, measured in the forward direction, of a graphite surface (3 nm scan range) in a high-symmetry direction (period of 0.246 nm) at two different velocities of (a) 30 nm/s and (b) 7.5 nm/s. The signature of parallel atomic row is clearly visible in the upper panel and rather difficult to distinguish in the lower panel.

The primary experimental difficulty of most AFMs and FFMs in the measurement of friction at very low velocities is the combination of thermal drift and piezocreep in the precise position of the tip with respect to the surface and in the zero-point setting of the force detection system (in our case the interferometers). In our setup, we employed special home-built drift compensators, integrated into our detection electronics, to compensate the variation in the four interferometer signals caused by drift or creep. This has enabled us to measure spectacularly slow friction loops even at velocities down to 0.01 nm/s without any noticeable drift. Here we present friction forces measured between a tungsten tip and a graphite surface at velocities between 0.1 and 100 nm/s. The Tribolever used in these measurements had a lateral spring constant of 6.1 N/m, which combined with a relatively stiff tip to an effective lateral spring constant of 4.5 N/m. The normal load was kept constant at 3.7 nN and we scanned along the high-symmetry [1110] direction. In order to avoid graphite flakes getting attached to the tip while scanning, we used a freshly etched tungsten tip on a high-quality highly oriented pyrolytic graphite (HOPG) sample, with grain sizes of the order of millimeters. To minimize the effects of "third particles," in particular water from the ambient, we performed the experiments in a closed chamber, where the relative humidity was maintained below 1%, by continually flushing with dry nitrogen. The scan range was fixed at 3 nm and all force images are composed of 512×512 pixels.

Lateral force images at two different scan velocities of 30 and 7.5 nm/s are shown in Fig. 8. The atomic rows can be recognized vaguely, but that information is washed out to a large extent by the thermal noise, especially at the lower velocity. The difference in the atomic contrast is also seen in the individual force loops at these two velocities, as is illustrated in Figs. 9(a) and 9(b), which further show that the stick-slip motion is much more irregular at the lower of these two velocities. Figure 9 also demonstrates that when we reduce the velocity, the area enclosed in the lateral force loops shrinks significantly. In other words, the average friction force is reduced to a near-zero value. At the lower velocity of 0.6 nm/s [Fig. 9(c)] the character of the motion has changed completely. It is hard to recognize any atomic periodicity. The noise shows that the tip makes frequent forward and

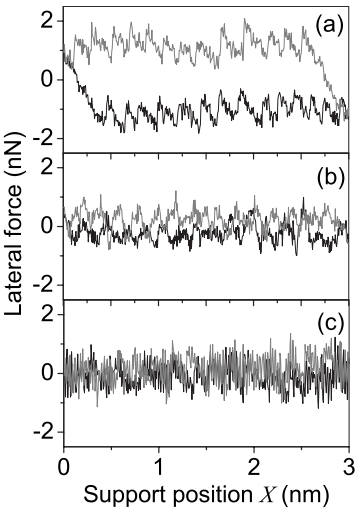

FIG. 9. Three characteristic friction loops at velocities of (a) 30 nm/s, (b) 7.5 nm/s, and (c) 0.6 nm/s. The area enclosed in the force loops reduces to almost zero as the velocity is reduced. At lower velocities, multiple peaks can be seen, corresponding to the multiple backward and forward jumps of the tip. This is a direct demonstration of the three regimes of (a) regular stick slip, (b) stochastic stick slip, and (c) thermal drift motion.

backward jumps. Together, Figs. 9(a)–9(c) illustrate three of the friction regimes discussed above, namely, regular stick slip, stochastic stick slip, and thermal drift. It is worth noting that in this experiment, the normal load is constant and there is no geometrical variation that could introduce changes in the corrugation of the potential.

As discussed above, the two-dimensional structure of the surface leads to distinct variations in the potential-energy corrugation as a function of the precise location of the scan line on the surface. These variations are particularly strong when the scan direction is aligned with one of the crystallographic directions of the substrate, as is the case here. Such effects have been reported recently by Schirmeisen *et al.*[8] on a graphite lattice. This variation and the corresponding periodic variation in the observed stick-slip period were already discussed briefly in Sec. IV A, where we used only a selection of force loops, corresponding to single-period one-dimensional-type trajectories over the two-dimensional surface. Here, it serves another purpose, namely, to extract a series of points of a $F_{\mathrm{fric}}(\gamma)$ curve from a single lateral force image; we use the force maxima in each individual force loop in the image to obtain a (lower) estimate of γ and the friction force F_{fric} is the average lateral force in the loop. Due to the variation in potential-energy corrugation from scan line to scan line, this procedure results in a comfortably wide range of γ values for which the friction force is obtained from a single force image.

The result of this analysis is shown in Fig. 10 for three velocities. The velocity plays a significant role, much stronger than could have been anticipated on the basis of a logarithmic dependence. For the lower velocity of 0.6 nm/s the friction force is found to approach zero at a high relative corrugation between $\gamma=5$ and $\gamma=6$.

Figure 10 also shows three fits with our model to the data sets for the three different velocities. In each curve, there has

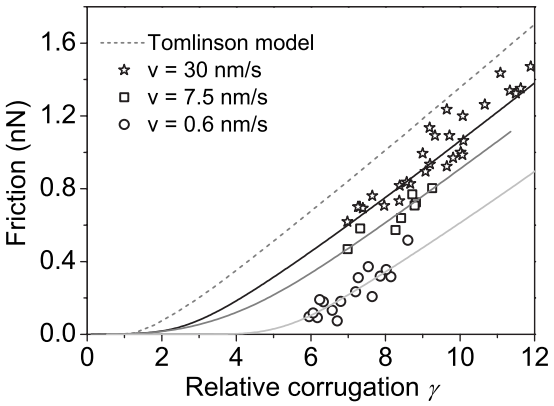

FIG. 10. Friction versus relative corrugation plotted together with theoretical curves. The symbols represent experimental data at 30 nm/s (stars), (b) 7.5 nm/s (squares), and (c) 0.6 nm/s (circles), which correspond to the stick-slip, stochastic, and thermal drift regimes of thermal activation. The dotted gray line is the friction according to the Tomlinson model (Ref. 2) and the three solid lines fitting the data at the three velocities are the results from numerical calculations using our thermolubricity model (see text).

been only a single free parameter, which was the pre-exponential factor ν, which we have associated before (Fig. 7) with the eigenfrequency of the Tribolever. In order to obtain a good fit in Fig. 10, we have been forced to use three very different values for ν at the three velocities; the best-fit value of ν changes by 2 orders of magnitude between the three curves, indicating that the measured velocity dependence is significantly stronger than the model predicts. The highest ν value is as much as 3 orders of magnitude above the resonance frequency of the Tribolever, which shows that something else than the eigenfrequency of the sensor is determining the attempt frequency for the thermal jumps.

V. SUMMARY AND CONCLUDING REMARKS

In this paper we have presented the combination of a simple rate-equation theory and measurements of the velocity dependence of atomic-scale friction between a graphite surface and a tungsten tip, either bare or dressed with a graphite flake. Particular attention has been paid both in the theory and in the experiment to the regime of ultralow velocities where the thermolubricity effect of thermal excitations completely dominates the motion of the tip. In addition to the range of velocities where the tip performs early precritical jumps over the energy barriers, which leads to a modest logarithmiclike reduction in the friction force, we identify an ultralow-velocity regime where the friction force scales linearly with velocity and it vanishes in the limit of zero velocity.

Although our one-dimensional theory provides an excellent fit to the corrugation dependence of the friction force at each separate velocity, it does not allow us to obtain a reasonable simultaneous fit for all velocities. The only free parameter in the model, which is the pre-exponential factor (attempt frequency) ν for thermally activated jumps, has to be chosen different for each velocity and typically it is well

above the resonance frequency of our cantilever.

For this interesting "discrepancy" we suggest three potential causes. The first of these lies in the strict one-dimensional nature of the model. Even though we have selected "one-dimensional geometries" in the experiment, by aligning the scan direction with easy sliding directions on the graphite crystal and by selecting measured force loops with a single spatial frequency, the tip still has the freedom to make sideways excursions during its sliding trajectory, which should lower the average friction force by an amount that may depend on the velocity. This point will be addressed in a separate publication.

The second effect that introduces a difference between model and measurement is the rapid dynamics of the tip apex, which has not been accounted for in this theory, in which the force detection system (tip plus cantilever) was assumed to respond as a single spring and the damping was assumed to be high. In a series of recent publications we have addressed the friction regimes and the extreme friction lowering introduced by the cantilever-plus-flexible-tip combination in a one-dimensional two-mass-two-spring model of the FFM experiment, in which the motion of the tip apex is characterized by a high attempt rate in the gigahertz regime.[14–16]

The third element is related to a potentially serious flaw in our analysis of the experimental force loops. As we mentioned in Sec. IV A, we have used the highest force maxima in the friction loops to obtain an estimate of the relative corrugation γ, and the precritical nature of the jumps renders this apparent γ a *lower* estimate of the true corrugation. A preliminary numerical analysis indicates that the error introduced by this procedure can be far from small, possibly making us underestimate γ by as much as a factor 2 or more. Since the corrugation appears in the argument of an exponential function [Eq. (1)], such an error introduces a gross underestimation of the thermal effect at play in most FFM measurements: this easily goes unnoticed since low values of the friction force appear to be correlated naturally with low corrugations of the potential. Further experimental and theoretical work is in progress to address this issue.

*Present address: NXP Semiconductors, HTC4, 5656 AE, Eindhoven, The Netherlands.

†Present address: Institute of Physical Chemistry, Russian Academy of Sciences, Leninsky prospect 31, 119991 Moscow, Russia.

‡Present address: Fraunhofer-Institut für Werkstoffmechanik IWM, Woehlerstr. 11, 79108 Freiburg, Germany.

§Corresponding author; frenken@physics.leidenuniv.nl

[1] L. Prandtl, Z. Angew. Math. Mech. **8**, 85 (1928).

[2] G. A. Tomlinson, Philos. Mag. **7**, 905 (1929).

[3] J. N. Glosli and G. M. McClelland, Phys. Rev. Lett. **70**, 1960 (1993).

[4] E. Gnecco, R. Bennewitz, T. Gyalog, Ch. Loppacher, M. Bammerlin, E. Meyer, and H.-J. Güntherodt, Phys. Rev. Lett. **84**, 1172 (2000).

[5] Y. Sang, M. Dube, and M. Grant, Phys. Rev. Lett. **87**, 174301 (2001).

[6] E. Riedo and E. Gnecco, Nanotechnology **15**, S288 (2004).

[7] E. Riedo, E. Gnecco, R. Bennewitz, E. Meyer, and H. Brune, Phys. Rev. Lett. **91**, 084502 (2003).

[8] A. Schirmeisen, L. Jansen, and H. Fuchs, Phys. Rev. B **71**, 245403 (2005).

[9] H. Dekker and A. Maassen van den Brink, Phys. Rev. E **49**, 2559 (1994).

[10] O. K. Dudko, A. E. Filippov, J. Klafter, and M. Urbakh, Chem. Phys. Lett. **352**, 499 (2002).

[11] M. Evstigneev and P. Reimann, Europhys. Lett. **67**, 907 (2004).

[12] S. Yu. Krylov, K. B. Jinesh, H. Valk, M. Dienwiebel, and J. W. M. Frenken, Phys. Rev. E **71**, 065101(R) (2005).

[13] M. Dienwiebel, G. S. Verhoeven, N. Pradeep, J. W. M. Frenken, J. A. Heimberg, and H. W. Zandbergen, Phys. Rev. Lett. **92**, 126101 (2004).

[14] S. Yu. Krylov and J. W. M. Frenken, New J. Phys. **9**, 398 (2007).

[15] D. G. Abel, S. Yu. Krylov, and J. W. M. Frenken, Phys. Rev. Lett. **99**, 166102 (2007).

[16] S. Yu. Krylov, J. A. Dijksman, W. A. van Loo, and J. W. M. Frenken, Phys. Rev. Lett. **97**, 166103 (2006).

[17] A. Socoliuc, R. Bennewitz, E. Gnecco, and E. Meyer, Phys. Rev. Lett. **92**, 134301 (2004).

[18] K. Shinjo and M. Hirano, Surf. Sci. **283**, 473 (1993).

[19] M. Hirano and K. Shinjo, Wear **168**, 121 (1993).

[20] M. Hirano, K. Shinjo, R. Kaneko, and Y. Murata, Phys. Rev. Lett. **78**, 1448 (1997).

[21] C. Daly, J. Zhang, and J. B. Sokoloff, Phys. Rev. E **68**, 066118 (2003).

[22] M. Dienwiebel, N. Pradeep, G. S. Verhoeven, H. W. Zandbergen, and J. W. M. Frenken, Surf. Sci. **576**, 197 (2005).

[23] M. Dienwiebel, E. de Kuyper, L. Crama, J. W. M. Frenken, J. A. Heimberg, D.-J. Spaanderman, D. Glastra van Loon, T. Zijlstra, and E. van der Drift, Rev. Sci. Instrum. **76**, 043704 (2005).

[24] T. Zijlstra, J. A. Heimberg, E. van der Drift, D. Glastra van Loon, M. Dienwiebel, L. E. M. de Groot, and J. W. M. Frenken, Sens. Actuators, A **84**, 18 (2000).